Chiral Gels

DOI: 10.1002/anie.201308554

Solvent-Driven Chiral-Interaction Reversion for Organogel Formation**

*Guangyan Qing, Xingxing Shan, Wenrui Chen, Ziyu Lv, Peng Xiong, and Taolei Sun**

Abstract: *For chiral gels and related applications, one of the critical issues is how to modulate the stereoselective interaction between the gel and the chiral guest precisely, as well as how to translate this information into the macroscopic properties of materials. Herein, we report that this process can also be modulated by nonchiral solvents, which can induce a chiral-interaction reversion for organogel formation. This process could be observed through the clear difference in gelation speed and the morphology of the resulting self-assembly. This chiral effect was successfully applied in the selective separation of quinine enantiomers and imparts "smart" merits to the gel materials.*

Chiral interaction is always a hot topic in chemistry because of its importance in biological processes,[1] medicine,[2] asymmetric catalysis,[3] and separation,[4] among other areas. An important challenge, and a new and promising direction of research on chiral materials and their applications, is how to transfer the weak chiral-interaction signal to changes in the macroscopic properties of materials,[5] for example, gelation and wettability. This process normally requires the participation of chiral guests or other asymmetric factors,[6] which can influence the assembly behavior of chiral aggregates or the conformation of chiral polymers and thus induce changes in the macroscopic properties of materials. Herein, we show that this process can also be modulated by nonchiral factors.[7] We report the ability of nonchiral solvents to trigger the reversion of chiral interactions for organogel formation. A mechanistic study indicated that solvents with different polarities determine the optimal conformations of chiral gelators and can unexpectedly initiate reverse interaction processes with chiral drug enantiomers. This finding not only enables a better understanding of the assembly behavior of chiral gelators, but can also be used to add new "smart" features to organogels.[8] We further demonstrate controllable enantiomeric separation based on this effect by the use of a semipermeable membrane modified with our chiral organogel. This membrane enables the selective permeation of L or D enantiomers through alteration of the polarity of the solvent.

Because of their reversible swelling and shrinkage properties, controllable assembly behavior, and broad application prospects in chirality-related domains, chiral organogels or hydrogels have received considerable attention in recent years.[9] For this study, dipeptides were chosen as the fundamental units for the construction of chiral gelators owing to their abundant hydrogen-bonding sites and programmable sequence combination. A *para*-disubstituted phenyl group was introduced as a bridge to connect two dipeptide arms and form a structure with C_2 symmetry to

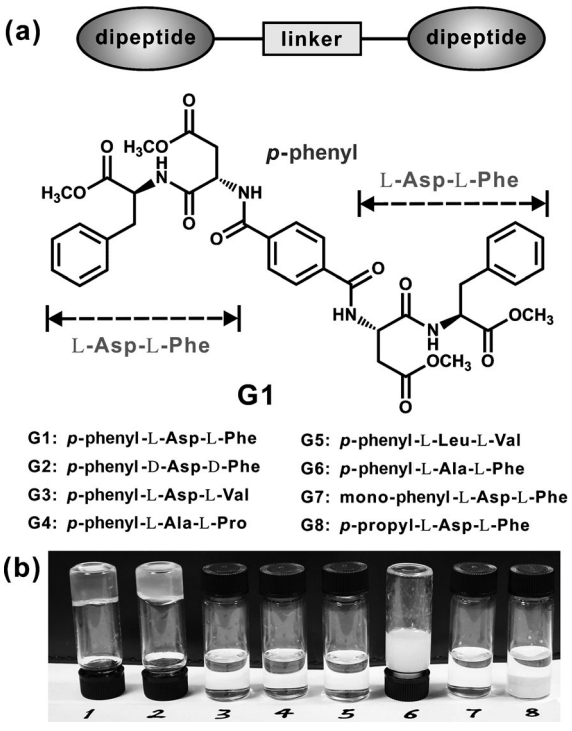

Scheme 1. a) Molecular design of small-molecular gelators **G1**–**G6** composed of two symmetrical dipeptide arms with different sequences linked to a rigid *p*-phenyl backbone; the structure of **G1** is shown as an example. **G7** and **G8** are controls with a one-arm or flexible-linkage architecture based on L-Asp-L-Phe. b) Photographs showing gel formation of **G1**–**G8** in ethanol after ultrasonic treatment for 4 min followed by cultivation at the normal temperature (20 °C) for 1 h.

[*] Prof. Dr. G. Qing,[+] X. Shan,[+] W. Chen, Z. Lv, P. Xiong, Prof. Dr. T. Sun
State Key Laboratory of Advanced Technology for Materials Synthesis and Processing, Wuhan University of Technology
122 Luoshi Road, Wuhan 430070 (P.R. China)
E-mail: suntl@whut.edu.cn

[+] These authors contributed equally.

[**] We thank the National Natural Science Foundation of China (21104061, 21275114, 91127027, 51173142) and the Major State Basic Research Development Program of China (973 Program; 2013CB933002) for funding. G. Qing acknowledges Hubei Provincial Department of Education for financial assistance through the "Chutian Scholar" program. We also thank Prof. J. Sun at Wuhan University for his help with theoretical calculations, and Dr. X. J. Wu for his help in the analysis of ^1H–^{13}C and ^1H–^1H COSY NMR spectra.

Supporting information for this article, including procedures for the synthesis of chiral gelators **G1**–**G8** and experimental details, is available on the WWW under http://dx.doi.org/10.1002/anie.201308554.

provide sufficient rigidity (Scheme 1 a). The relationship between the dipeptide sequence and the gelation capacity in ethanol was first explored. Six dipeptide sequences were examined, namely, L-Asp-L-Phe (in **G1**), D-Asp-D-Phe (in **G2**), L-Asp-L-Val (in **G3**), L-Ala-L-Pro (in **G4**), L-Leu-L-Val (in **G5**), and L-Ala-L-Phe (in **G6**), but only **G1**, **G2**, and **G6** formed a macroscopic organogel (Scheme 1 b). This result indicates that the Phe residue is necessary for gel formation. We presume that the π–π stacking between adjacent phenyl groups is a vital driving force for the supramolecular self-assembly of the gel in this case. Control experiments with single-arm (compound **G7**) or flexible structures (compound **G8**) based on L-Asp-L-Phe further proved the importance of a two-arm, rigid architecture for gelation. Our following research mainly focused on the gelator **G1** because of its excellent capacity for gel formation.

By conventional incubation, the gelation of **G1** is a slow process requiring almost 1 day for the formation of a macroscopic gel in ethanol (gelator concentration: 1 mg mL^{-1}). However, this process can be shortened significantly to about 1 h by brief ultrasonic treatment (4 min) before incubation at 20 °C (Figure 1 a).[10] Circular dichroism (CD) spectroscopy[11] was used to monitor this process (see Figure S1 in the Supporting Information).[12] The spectrum showed positive and negative "Cotton effect" bands with peaks at 290 and 310 nm, respectively. These bands were enhanced dramatically when the duration of ultrasonic treatment was increased from 10 s to 4 min. Our results showed the occurrence of a self-assembly process of **G1** from single molecules to supramolecular aggregates (Figure 1 a), which function as the seeds for further growth into long helical nanofibers, as shown by the atom force microscopic (AFM) image (bottom of Figure 1 a).

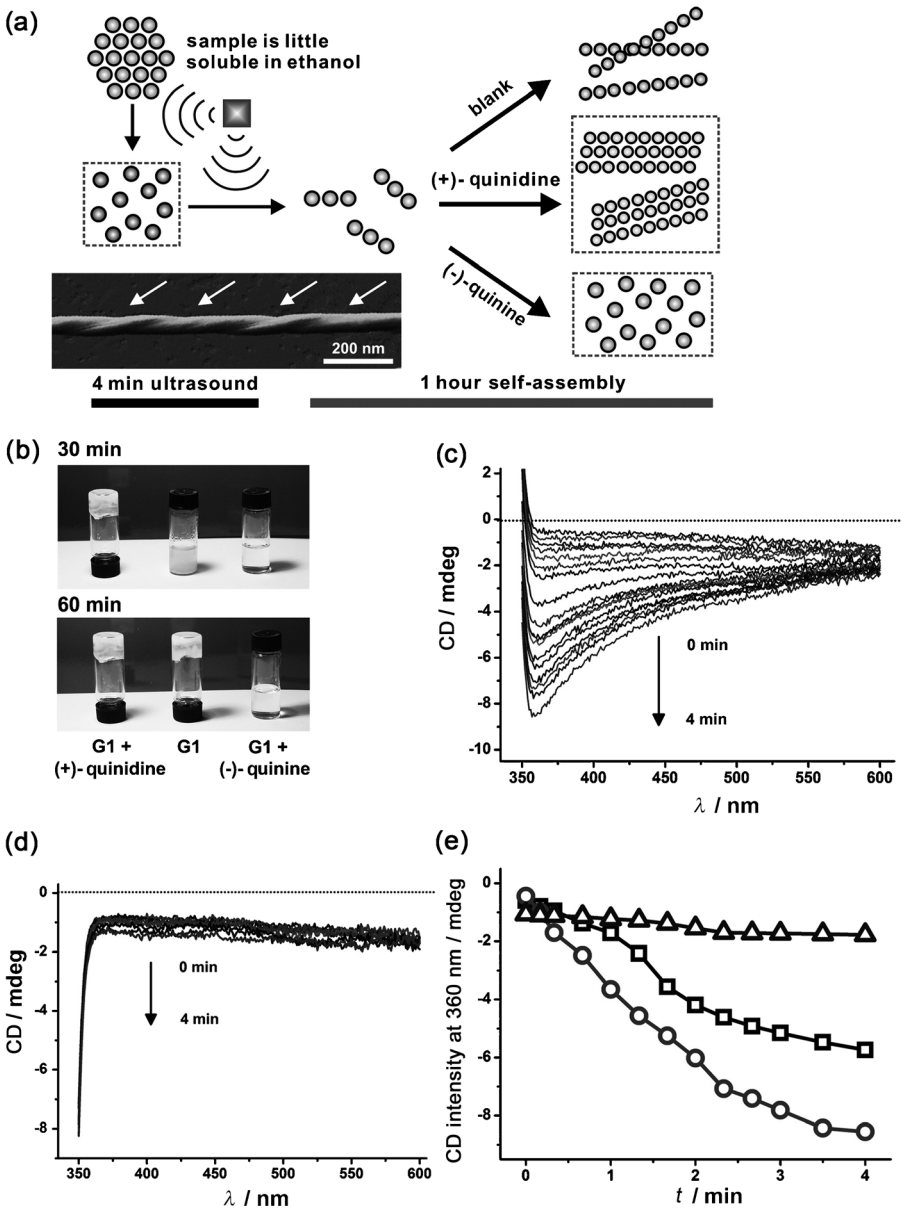

Figure 1. a) Illustration of the ultrasound-promoted self-assembly processes of **G1**, with or without the participation of quinine enantiomers. Ultrasonic treatment can accelerate the dissolution and dispersion of gelator molecules in ethanol, and the formation of supramolecular aggregates. The self-assembly process is strongly influenced by the configuration of quinine, which can initiate different processes. b) Photographs showing the states of gels at 30 and 60 min. c,d) CD spectra of **G1** exposed to ultrasonic treatment for different periods of time (0–4 min) with the addition of an equal amount of (+)-quinidine (c) or (−)-quinine (d) as a chiral guest. e) Comparison of the CD intensity ($\lambda = 360$ nm) with respect to ultrasonic-treatment time for **G1** (□), **G1** with (+)-quinidine (○), and **G1** with (−)-quinine (△).

Interestingly, this self-assembly process was significantly influenced by the addition of small-molecular chiral guests in the form of a pair of pseudoenantiomers: (+)-quinidine and (−)-quinine. The former is an antiarrhythmic drug, whereas the latter is well-known for its antipyretic, antimalarial, and anti-inflammatory properties.[13] It was found that the addition of (+)-quinidine could significantly accelerate gel formation: The gelation time was shortened from 1 h to 30 min (Figure 1 b). Scanning electronic microscopy (SEM) showed that in the presence of (+)-quinidine, the gel fibers become much wider and thicker (see Figure S2b) than the thin, long fibers formed from pure **G1** (see Figure S2a). However, a totally different situation was observed upon the addition of (−)-quinine, which strongly inhibited gel forma-

tion under the same conditions. The solution of **G1** after (−)-quinine addition remained in a liquid state after ultrasonic treatment and subsequent incubation for as long as 12 h (Figure 1b). The above results indicate that (+)-quinidine and (−)-quinine have opposite effects on the gel-formation process of **G1**. CD spectra revealed that (+)-quinidine (Figure 1c) or (−)-quinine (Figure 1d) directly determined the self-assembly of **G1** during the initial ultrasonic-treatment step. The addition of an equal amount of (+)-quinidine induced a clear enhancement of the CD signals, with a decrease in the intensity at 360 nm from −0.53 to −9.0 mdeg, whereas the chiral signal was strongly suppressed by the addition of (−)-quinine, and no apparent change was observed upon prolonged incubation. A comparison of the time dependence of the peak intensity at 360 nm (Figure 1e) clearly demonstrates the promotion and inhibition of the initial self-assembly process of **G1** by (+)-quinidine and (−)-quinine, respectively.

Solvent polarity is an important factor governing gel formation. We changed the solvent from ethanol to a weakly polar solvent—chloroform—and found that the macroscopic organogel could not form at a low concentration (below 10 mg mL^{-1}), even though we increased the incubation time and the temperature (see Figure S4). Therefore, AFM[14] was used to study the influence of (+)-quinidine and (−)-quinine on the self-assembly of **G1** in chloroform (CD spectra could not be obtained owing to the serious background noise in chloroform (see Figure S3c)). For pure **G1**, by adjusting the concentration of the gelator (e.g. 0.1, 0.5, 1.0, and 2.0 mg mL^{-1}) in chloroform, well-ordered micropatterns of single long fibers, dendritic patterns, and nestlike patterns could be clearly observed on mica (see Figure S5). These results indicate three different self-assembly behaviors of **G1** at low, medium, and high concentrations, which provide an ideal platform for studying the effect of (+)-quinidine and (−)-quinine. Unexpectedly, we observed an interesting effect that was totally opposite to that in ethanol.

At a concentration of 1.0 mg mL^{-1}, pure **G1** exhibited a nestlike microstructure (see Figure S5c). The addition of (+)-quinidine (0.4 equiv) to the solution of **G1** caused the collapse of this microstructure and the generation of many short and small fibers (Figure 2a,c), which even became much shorter and thinner when the molar ratio of (+)-quinidine to **G1** was increased to 1:1. This result indicates that (+)-quinidine can inhibit the self-assembly of **G1** in chloroform to a remarkable extent. However, the presence of (−)-quinine promoted the formation of fibers, which further assembled into large rootlike patterns (Figure 2b,d) upon an increase in the (−)-quinine concentration. The different effects of (+)-quinidine and (−)-quinine became much more distinct when the culture temperature was elevated to 30 °C. Under these conditions, the rootlike pattern grew rapidly from an average size of about 5 to about 30 μm in the presence of quinine (Figure 2f), whereas no evident change was observed with (+)-quinidine (Figure 2e). Meanwhile, this chiral discrimination remained even when the molar ratio was increased from 1:1 to 2:1 (see Figure S6).

CD spectra (see Figure S3) indicated that the absolute configurations of **G1**, (+)-quinidine, and (−)-quinine did not

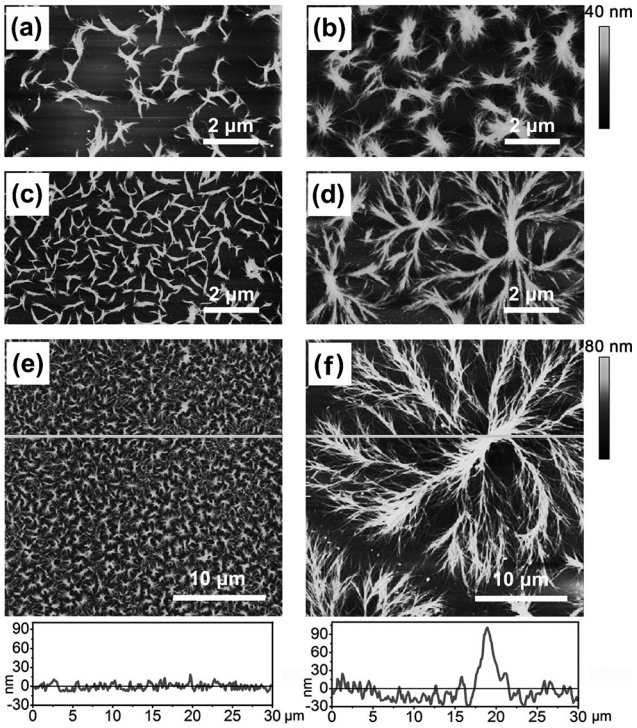

Figure 2. Morphology of self-assembled structures of **G1** on mica after incubation in chloroform with (+)-quinidine (a,c) or (−)-quinine (b,d) in different molar ratios at 20 °C for 1 h, as observed by AFM in the tapping mode. The molar ratio of the chiral guest to **G1** was 0.4:1 (a,b) or 1:1 (c,d). e,f) Large-scale morphologies of **G1** after incubation at 30 °C for 1 h with an equal molar amount of (+)-quinidine (e) or (−)-quinine (f), and the corresponding section profiles.

Table 1: Association constants (K_a) between chiral gelators **G1**–**G8** and (+)-quinidine or (−)-quinine in ethanol or chloroform at 20 °C.

Gelator	K_a in ethanol [L mol^{-1}][a]		$K_{(+)}/K_{(-)}$
	(+)-quinidine	(−)-quinine	
(L,L)-G1	[b]	$(1.42\pm0.20)\times10^3$	
(D,D)-G2	$(2.09\pm0.28)\times10^3$	$(4.80\pm0.57)\times10^2$	4.35
G3	$(1.60\pm0.32)\times10^3$	$(5.00\pm0.62)\times0^3$	1/3.12
G4	$(2.51\pm0.39)\times10^3$	$(3.41\pm0.31)\times10^3$	1/1.36
G5	$(1.08\pm0.13)\times10^4$	$(1.14\pm0.15)\times10^4$	1/1.05
G6	[b]	$(1.20\pm0.20)\times10^3$	
G7	[b]	$(5.88\pm0.65)\times10^3$	
G8	$(1.37\pm0.22)\times10^4$	$(1.44\pm0.18)\times10^4$	1/1.05
	K_a in chloroform [L mol^{-1}][a]		
(L,L)-G1	$(2.27\pm0.29)\times10^4$	$(5.82\pm0.39)\times10^3$	3.90
(D,D)-G2	$(6.30\pm0.75)\times10^3$	$(1.90\pm0.28)\times10^4$	1/3.01
G3	$(1.53\pm0.16)\times10^4$	$(9.50\pm1.10)\times10^3$	1.61
G4	$(7.70\pm0.98)\times10^4$	$(6.80\pm0.72)\times10^4$	1.13
G5	$(2.37\pm0.29)\times10^4$	$(2.33\pm0.27)\times10^4$	1.02
G6	$(1.86\pm0.49)\times10^4$	$(4.00\pm0.21)\times10^3$	4.65
G7	$(3.45\pm0.41)\times10^4$	$(1.16\pm0.09)\times10^4$	2.97
G8	$(4.80\pm0.58)\times10^3$	$(4.02\pm0.46)\times10^3$	1.19

[a] K_a values were obtained from fluorescence titration experiments according to intensity changes in the emission-peak maximum. [b] A K_a value could not be obtained because the change in the spectrum was too small.

change under the experimental conditions. Therefore, the above results reveal the uncommon phenomenon of a reversion triggered by solvent polarity (which is itself a non-asymmetric factor) of a chiral interaction for organogel formation. To explore the molecular mechanism, we conducted fluorescence titration experiments[15] to obtain the association constants (K_a) between **G1** and (+)-quinidine or (−)-quinine in ethanol and chloroform. **G1** exhibited strong complexation with (−)-quinine in ethanol and induced a 60% increase in the fluorescence intensity (see Figure S7b), thus resulting in a K_a value of 1300 L mol^{-1} (Table 1). As a result, the self-assembly process of **G1** is strongly suppressed by competitive complexation with (−)-quinine. By contrast, the addition of (+)-quinidine induced almost no change in the spectrum, thus indicating a very weak host–guest combination. This result is in good agreement with the gelation performance in ethanol. To elucidate the importance of chirality, we used a reference compound, (D,D)-**G2**, which exhibited much stronger complexation with (+)-quinidine than with (−)-quinine, thus resulting in a $K_{(+)}/K_{(-)}$ ratio of 4.35 (see Figure S8). These data prove the relevance of the chiral interaction. Similarly, we also investigated the chiral interaction in chloroform. Contrary to that in ethanol, **G1** exhibited a much stronger complexation with (+)-quinidine than with (−)-quinine, and the $K_{(+)}/K_{(-)}$ ratio was 3.90. These data provide solid evidence that enables a better understanding of the solvent-driven reversion of the chiral interaction.

We also investigated the relationship between the dipeptide sequence and the observation of chiral-interaction reversion. By comparing the binding properties of various chiral gelators (**G3**–**G8**) with quinine pseudoenantiomers in ethanol or chloroform, we found that the dipeptides containing Asp or Phe units (**G1**, **G2**, **G3**, **G6**, and **G7**) usually had a stronger chiral-discrimination ability than that of dipeptides composed of other amino acids (**G4** and **G5**). Moreover, in ethanol, all exhibited larger association constants with (−)-quinine than with (+)-quinidine ($K_{(+)}/K_{(-)}$ ratios smaller than 1), whereas in chloroform, the $K_{(+)}/K_{(-)}$ ratio was always larger than 1 (Table 1). The analysis of these data indicates that this effect not only exists for a specific dipeptide sequence (Asp-Phe), but may be a rather general effect valid for many other peptides. It may thus provide a wide selection range for materials design. Nevertheless, the rigidity of the structure is also critical for chiral discrimination. This ability was almost lost in gelator **G8** in which the rigid *para*-phenyl linkage was replaced with a flexible alkane chain: a result that is also consistent with its gelation behavior.

The mechanism of the reversion of the chiral interaction was further studied by quantum-chemical calculations at the single-molecule level (Gaussian 2003, density functional theory at the 6-311g(d) level).[16] First, the optimum conformations of **G1** in ethanol or chloroform were obtained (see Figure S9; their possible self-assembly modes are discussed briefly in Figure S10). Since both (+)-quinidine and (−)-quinine have bulky naphthalene units with strong π–π-stacking capacity, these model analyses revealed the critical role of π–π stacking between aromatic rings in the promotion and inhibition of **G1** assembly and the gel-formation process. This hypothesis was first proved by a control experiment in which quinoline alone was introduced as a guest; quinoline completely inhibited (Figure 3a) the formation of gel fibers in chloroform (see Figure S11).

Figure 3b–e shows the calculated interaction models of **G1** with (+)-quinidine or (−)-quinine. In ethanol, (−)-quinine combines with **G1** strongly (Figure 3c) through both H bonds (green dashed lines) and π–π stacking (red arrow) between its naphthalene ring and the phenyl group of **G1**, owing to the conformational compatibility between the two molecules. In contrast, (+)-quinidine binds to **G1** weakly

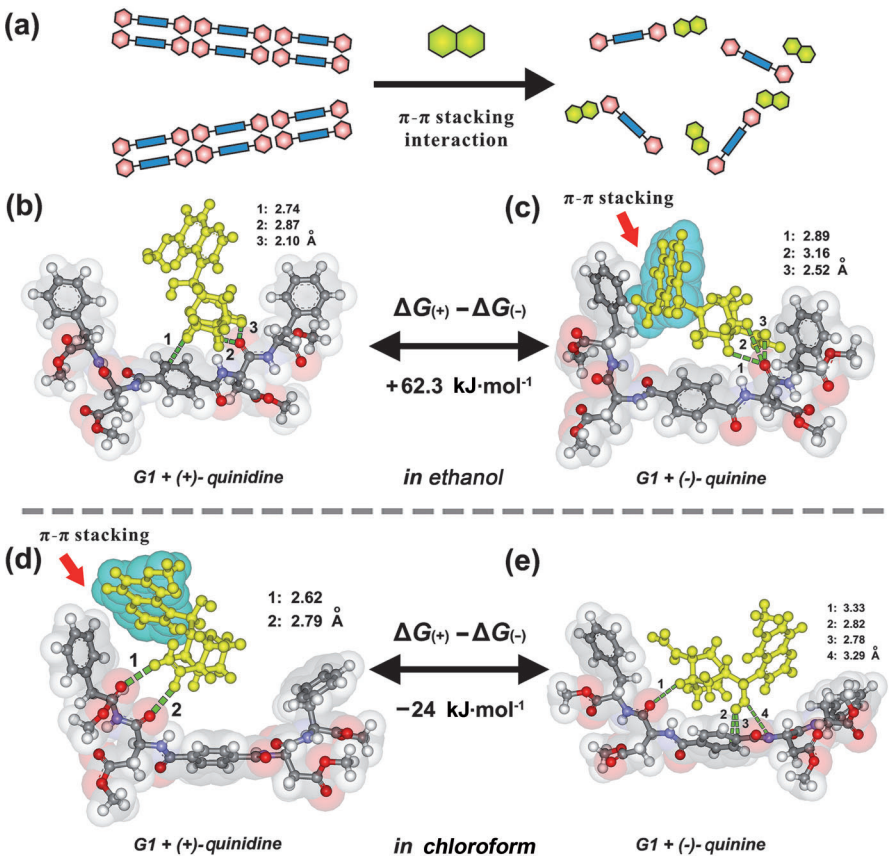

Figure 3. a) Illustration of the quinolone-inhibited self-assembly of **G1**. b–e) Molecular-interaction models of **G1** with (+)-quinidine or (−)-quinine in ethanol (b,c) or chloroform (d,e). The π–π stacking between quinoline (highlighted by the blue electronic cloud) and the adjacent phenyl group is indicated by red arrows, whereas H bonding is indicated by green dashed lines with different bond lengths.

only through H bonds (green dashed lines, Figure 3b) owing to the mismatched conformations. Stronger complexation of **G1** with (−)-quinine gives rise to a binding free energy (ΔG) much lower than that with (+)-quinidine; their difference ($\Delta G_{(+)} - \Delta G_{(-)}$) is $+62.3\ \mathrm{kJ\,mol^{-1}}$. The strong combination between **G1** and (−)-quinine, as well as the occupation of π–π interaction sites, prevents **G1** molecules from assembling with each other, and finally inhibits gel formation. However, the weak interaction with (+)-quinidine leads to a more extended conformation of **G1**, and an extra unoccupied aromatic quinolone ring, which can enhance the π–π stacking of **G1** molecules and thus promote the self-assembly process. Interestingly, in chloroform, the conformation selectivity between **G1** and (+)-quinidine/(−)-quinine is just the opposite ($\Delta G_{(+)} - \Delta G_{(-)} = -24.0\ \mathrm{KJ\,mol^{-1}}$; Figure 3d,e), in close agreement with the experimental results of the assembly behavior. Intermolecular π–π stacking was proved by the ^{1}H–^{13}C COSY NMR spectra (see Figure S12), in which clear coupling and overlap occur between signals of the aromatic rings of **G1** and those of the naphthalene ring of (+)-quinidine. Moreover, multiple H-bonding interactions may also contribute to this process, as shown by the ^{1}H–^{1}H COSY NMR spectra (see Figure S13).

The effect of this stereoselective interaction between **G1** and chiral guests, which can be completely reversed by different solvents, may be very useful in chiral separation and other applications. To address this point, we designed a device composed of a dialysis membrane (typical molecular-weight cutoff: 3500) on which organogels of **G1** were immobilized.[17] The permeation of (+)-quinidine and (−)-quinine through the membranes was then evaluated in a medium of either ethanol or chloroform. In ethanol (Figure 4a), (+)-quinidine exhibited fast permeation behavior, and the permeation fraction (PF, refers to the percentage of compound permeated out) increased rapidly to about 60% in 2 h. By contrast, the permeation of (−)-quinine was much slower, and the PF value only reached about 20% in 2 h, and gradually increased to about 40% after 4 h. In contrast, when the medium was changed to chloroform (Figure 4b), the permeation of (−)-quinine became much faster than that of (+)-quinidine, and the PF values were 80 and 10%, respectively, after permeation for 1 h. These results indicate excellent chirality-selective permeation behavior of the membrane, whereby the selectivity can be controlled and reversed by the application of a particular solvent. In a further study with racemic quinine, a final proportion of 6:1 for (+)-quinidine and (−)-quinine was obtained after a single permeation process in ethanol (Figure 4c), thus proving the feasibility of this device in chiral separation.

In conclusion, we have described herein an interesting effect of solvent-triggered chiral-interaction reversion, which directly determines organogel- and microstructure-formation processes. This effect has advantages over conventional routes based on asymmetric factors for the translation of chiral-interaction signals into macroscopic materials properties and adds new "smart" features to organogels. It may thus provide important insight into the design of chiral gels and relevant applications,[18] such as enantiomeric separation.

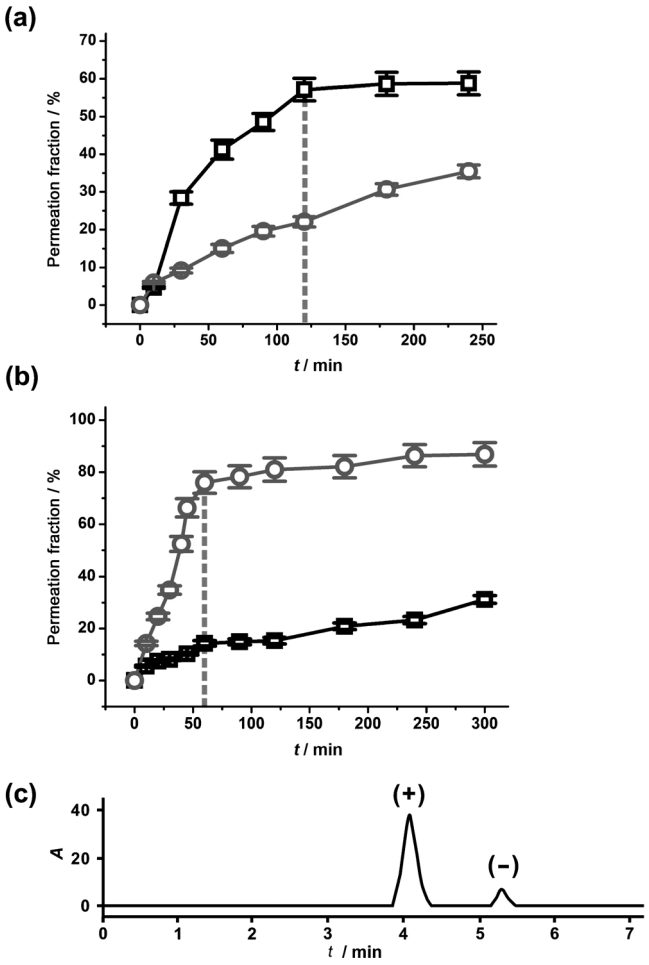

Figure 4. a,b) Selective permeation behavior of the **G1**-modified dialysis membrane for quinine pseudoenantiomers in ethanol (a) or chloroform (b). Black squares: (+)-quinidine; gray circles: (−)-quinine. c) HPLC chromatogram for the enantioseparation profile of a quinine racemate.

Received: October 1, 2013
Revised: December 17, 2013
Published online: January 21, 2014

Keywords: chiral gels · chiral recognition · host–guest systems · self-assembly · solvent effects

[1] a) T. D. James, K. R. A. Samankumara Sandanayake, S. Shinkai, *Nature* **1995**, *374*, 345–347; b) M. Kato, N. Matsumoto, K. K. Sakai, T. Toyóoka, *J. Pharm. Biomed. Anal.* **2003**, *30*, 1845–1850; c) A. Kühnle, T. R. Linderoth, B. Hammer, F. Besenbacher, *Nature* **2002**, *415*, 891–893.
[2] P. D. Thornton, R. J. Mart, R. V. Ulijn, *Adv. Mater.* **2007**, *19*, 1252–1256.
[3] S. C. Mohapatra, J. T. Hsu, *Biotechnol. Bioeng.* **1999**, *64*, 213–220.
[4] M. Kato, K. K. Sakai, N. Matsumoto, T. Toyóoka, *Anal. Chem.* **2002**, *74*, 1915–1921.
[5] a) W. J. Chung, J. W. Oh, K. Kwak, B. Y. Lee, J. Meyer, E. Wang, A. Hexemer, S. W. Lee, *Nature* **2011**, *478*, 364–368; b) J. J. D. de Jong, T. D. Tiemersma-Wegman, J. H. van Esch, B. L. Feringa, *J. Am. Chem. Soc.* **2005**, *127*, 13804–13805; c) W. Weng,

J. B. Beck, A. M. Jamieson, S. J. Rowan, *J. Am. Chem. Soc.* **2006**, *128*, 11663 – 11672; d) G. Y. Qing, T. L. Sun, *NPG Asia Mater.* **2012**, *4*, e4.

[6] a) D. K. Smith, *Chem. Soc. Rev.* **2009**, *38*, 684 – 694; b) C. S. Love, A. R. Hirst, V. Chechik, D. K. Smith, I. Ashworth, C. Brennan, *Langmuir* **2004**, *20*, 6580 – 6585; c) X. Q. Dou, P. Li, D. Zhang, C. L. Feng, *Soft Matter* **2012**, *8*, 3231 – 3238; d) A. R. Hirst, B. Q. Huang, V. Castelletto, I. W. Hamley, D. K. Smith, *Chem. Eur. J.* **2007**, *13*, 2180 – 2188; e) M. M. Smith, W. Edwards, D. K. Smith, *Chem. Sci.* **2013**, *4*, 671 – 676; f) S.-i. Sakurai, K. Okoshi, J. Kumaki, E. Yashima, *J. Am. Chem. Soc.* **2006**, *128*, 5650 – 5651; g) Y. Fu, B. Li, Z. Huang, Y. Li, Y. Yang, *Langmuir* **2013**, *29*, 6013 – 6017; h) W. G. Miao, L. Zhang, X. F. Wang, L. Qin, M. H. Liu, *Langmuir* **2013**, *29*, 5435 – 5442.

[7] a) R. Iwaura, T. Shimizu, *Angew. Chem.* **2006**, *118*, 4717 – 4720; *Angew. Chem. Int. Ed.* **2006**, *45*, 4601 – 4604; b) J. Jiang, T. Y. Wang, M. H. Liu, *Chem. Commun.* **2010**, *46*, 7178 – 7180; c) B. V. Shankar, A. Patnaik, *J. Phys. Chem. B* **2007**, *111*, 9294 – 9300.

[8] a) M. A. Cohen Stuart, W. T. S. Huck, J. Genzer, M. Müller, C. Ober, M. Stamm, G. B. Sukhorukov, I. Szleifer, V. V. Tsukruk, M. Urban, F. Winnik, S. Zauscher, I. Luzinov, S. Minko, *Nat. Mater.* **2010**, *9*, 101 – 113; b) P. M. Mendes, *Chem. Soc. Rev.* **2008**, *37*, 2512 – 2529; c) A. Pranzetti, S. Mieszkin, P. Iqbal, F. J. Rawson, M. E. Callow, J. A. Callow, P. Koelsch, J. A. Preece, P. M. Mendes, *Adv. Mater.* **2013**, *25*, 2181 – 2185; d) G. Y. Li, L. Q. Shi, R. J. Ma, Y. L. An, N. Huang, *Angew. Chem.* **2006**, *118*, 5081 – 5084; *Angew. Chem. Int. Ed.* **2006**, *45*, 4959 – 4962; e) J. R. Capadona, K. Shanmuganathan, D. J. Tyler, S. J. Rowan, C. Weder, *Science* **2008**, *319*, 1370 – 1374.

[9] a) X. H. Yan, P. L. Zhu, J. B. Li, *Chem. Soc. Rev.* **2010**, *39*, 1877 – 1890; b) A. V. Kabanov, S. V. Vinogradov, *Angew. Chem.* **2009**, *121*, 5524 – 5536; *Angew. Chem. Int. Ed.* **2009**, *48*, 5418 – 5429; c) L. E. Buerkle, S. J. Rowan, *Chem. Soc. Rev.* **2012**, *41*, 6089 – 6102.

[10] a) Y. B. He, Z. Bian, C. Q. Kang, R. Z. Jin, L. X. Gao, *New J. Chem.* **2009**, *33*, 2073 – 2080; b) G. D. Liang, J. T. Xu, X. S. Wang, *J. Am. Chem. Soc.* **2009**, *131*, 5378 – 5379.

[11] a) G. Gottarelli, S. Lena, S. Masiero, S. Pieraccini, G. P. Spada, *Chirality* **2008**, *20*, 471 – 485; b) L. Z. Zhao, R. Xiang, R. J. Ma, X. Wang, Y. L. An, L. Q. Shi, *Langmuir* **2011**, *27*, 11554 – 11559.

[12] J. Makarević, M. Jokić, Z. Raza, Z. Štefanić, B. Kojić-Prodić, M. Žinić, *Chem. Eur. J.* **2003**, *9*, 5567 – 5580.

[13] H. Suzuki, H. Onishi, Y. Takahashi, M. Iwata, Y. Machida, *Int. J. Pharm.* **2003**, *251*, 123 – 132.

[14] a) A. R. Hirst, S. Roy, M. Arora, A. K. Das, N. Hodson, P. Murray, S. Marshall, N. Javid, J. Sefcik, J. Boekhoven, J. H. van Esch, S. Santabarbara, N. T. Hunt, R. V. Ulijn, *Nat. Chem.* **2010**, *2*, 1089 – 1094; b) X. Li, K. L. Liu, J. Li, E. P. S. Tan, L. M. Chan, C. T. Lim, S. H. Goh, *Biomacromolecules* **2006**, *7*, 3112 – 3119; c) G. Y. Qing, H. Xiong, F. Seela, T. L. Sun, *J. Am. Chem. Soc.* **2010**, *132*, 15228 – 15232.

[15] a) L. Pu, *Chem. Rev.* **2004**, *104*, 1687 – 1716; b) P. A. Gale, S. E. García-Garrido, J. Garric, *Chem. Soc. Rev.* **2008**, *37*, 151 – 190.

[16] a) D. S. Sholl, J. A. Steckel, *Desnity Functional Theory*, Wiley-VCH, Hoboken, **2009**; b) T. Muraoka, K. Kinbara, Y. Kobayashi, T. Aida, *J. Am. Chem. Soc.* **2003**, *125*, 5612 – 5613.

[17] a) Y. P. Wang, H. P. Xu, X. Zhang, *Adv. Mater.* **2009**, *21*, 2849 – 2864; b) P. A. Gale, R. Quesada, *Coord. Chem. Rev.* **2006**, *250*, 3219 – 3244; c) J. Zhou, M. Pita, M. Motornov, E. Katz, S. Minko, *ACS Appl. Mater. Interfaces* **2009**, *1*, 532 – 536.

[18] a) D. Díaz Díaz, D. Kühbeck, R. J. Koopmans, *Chem. Soc. Rev.* **2011**, *40*, 427 – 448; b) D. J. Beebe, J. S. Moore, J. M. Bauer, Q. Yu, R. H. Liu, C. Devadoss, B. H. Jo, *Nature* **2000**, *404*, 588 – 590; c) S. E. Chung, W. Park, S. Shin, S. A. Lee, S. Kwon, *Nat. Mater.* **2008**, *7*, 581 – 587.

